

## MOLECULAR DOCKING AND INTERACTION OF COUMARIN DERIVATIVES AS INHIBITORS OF GROWTH FACTOR RECEPTORS

FAHIKA NAZEERULLA\*

Department of Biotechnology, Ramaiah University of Applied Sciences, Bengaluru, Karnataka, India. Email: fahikanazeerulla@gmail.com

Received: 30 January 2023, Revised and Accepted: 15 February 2023

### ABSTRACT

**Objective:** Cancer is the largest cause of mortality in the globe, accounting for over 10 million deaths in 2020, or roughly one in every six. Because growth factor receptors are involved in the pathophysiology of the disease in several ways, human epidermal growth factors (HER-2 and HER-3) and vascular endothelial growth factor receptors (VEGFR-2 and VEGFR-3) might be as considered therapeutic targets. Coumarins and derivatives were chosen for this study to investigate their pharmacological characteristics and therapeutic effect against the targeted proteins implicated in the pathogenesis of different cancers.

**Methods:** In this work, 50 coumarins and their derivatives were chosen to assess their binding affinity with the targeted proteins (HER-2, HER-3, VEGFR-2, and VEGFR-3). PyRx, a virtual tool, was utilized to perform molecular docking. The investigation was carried out computationally, with data and molecular structures of the phytochemicals and proteins derived from Indian medicinal plants, phytochemistry, and therapeutics, as well as PubChem. The protein structure was validated using a variety of tools, including Protein Data Bank sum generate and BIOVIA discovery studio software. The pharmacological assessment of the ligands was carried out using ADMET filters.

**Results:** According to the results of molecular docking, the ligands Glycycoumarin, Mutisifurocoumarin, Thunberginol A, Pervilleanine, Licocoumarin A, and Murrayacoumarin C had the lowest binding affinity toward the four targeted proteins.

**Conclusion:** Since these compounds are effective against the growth factor receptors implicated in cancer pathogenesis, they could be a suitable candidate for cancer management and suppression. However, *in vitro* research is still required to support these findings.

**Keywords:** Molecular docking, Vascular endothelial growth factor receptor, Human epidermal growth factor receptor, Coumarin, Cancer, ADMET analysis, Phytochemicals, Tyrosine kinases pathway.

© 2023 The Authors. Published by Innovare Academic Sciences Pvt Ltd. This is an open access article under the CC BY license (<http://creativecommons.org/licenses/by/4.0/>) DOI: <http://dx.doi.org/10.22159/ijms.2023v11i2.47145>. Journal homepage: <https://innovareacademics.in/journals/index.php/ijms>

### INTRODUCTION

In the current age of consumerism, the alarming trend of ultra-processed foods, lifestyle, and the ignorant use of carcinogens in several products used in daily life has turned cancer from a very dangerous disease, that used to be an unlikely occurrence, to a much more potent danger that occurs at a greatly increased frequency. Cancer is a complex illness that primarily affects persons over the age of 50. However, evidence suggests that the incidence of cancers of various organs has been increasing in many parts of the world in adults under the age of 50 [1]. In light of recent developments, the significance of even the smallest results supporting the fight against cancer has greatly increased [2].

To fight the titan known as cancer it is important to select a means to target cancer. The greater the importance of the target in the functioning of cancer cells, the greater the efficiency of the treatment in cancer reduction. Hence, we have selected human epidermal growth factor receptor 2 (HER2), which has been shown to strongly promote carcinogenesis, HER3 which interacts with another receptor tyrosine kinase (RTK), such as HER2, to activate various pathways, and vascular endothelial growth factor receptor (VEGFR2) whose overexpression increases cellular proliferation and invasion and tumor formation and Finally, VEGFR-3 which is involved in numerous kinds of solid tumors increasing cancer cell motility and invasion, facilitating cancer cell metastasis.

HER2 is a protein that helps govern cell development and is encoded by the ERBB2 gene in humans. The HER2 gene mutates (alters) and duplicates. When this happens, the ERBB2 produces an excessive amount of HER2 protein, leading cells to divide, and expand too quickly. In these malignancies, the major mechanism of HER2 activation is HER2

gene amplification, which results in total HER2 protein overexpression on the cellular membrane [3,4]. The majority of HER2 mutations are of the activating type, and they arise in the absence of simultaneous HER2 gene amplification [5].

HER3 is another member of the HER family (HER-3). It was originally thought that HER-3 lacked tyrosine kinase and catalytic activity and that its intracellular portion could not bind ATP or be auto-phosphorylated [6]. The biochemical study has established that the HER-3 kinase domain is a particular allosteric activator, acting as a functional activator to activate the recipient kinase. Overexpression of HER3 increases tumor growth by increasing metastatic potential, and it is a key cause of therapy failure in several human malignancies [7].

One of the two tyrosine kinase receptors involved in angiogenesis is VEGFR2. When triggered by its ligand VEGF, VEGFR2 stimulates the creation of neighboring vessels, allowing growth hormones, nutrients, and oxygen to be delivered to cancer cells for proliferation, migration, metastasis, and survival. Angiogenesis driven by VEGF and VEGFR2 contributes to the aggressive natures of various cancers and leads to a high mortality rate [8,9].

Finally, VEGFR3 tyrosine kinase is mostly expressed in lymphatic vessels. VEGFR3 is involved in the biology and pathophysiology of the lymphatic vasculature, as well as signaling lymphatic endothelial migration, survival, and proliferation. VEGFR-3 plays an essential role in leukemic cell proliferation, survival, and treatment resistance [10].

Curcumin is a brilliant yellow compound generated by the *Curcuma longa* plant species. It is the main curcuminoid in turmeric, which is

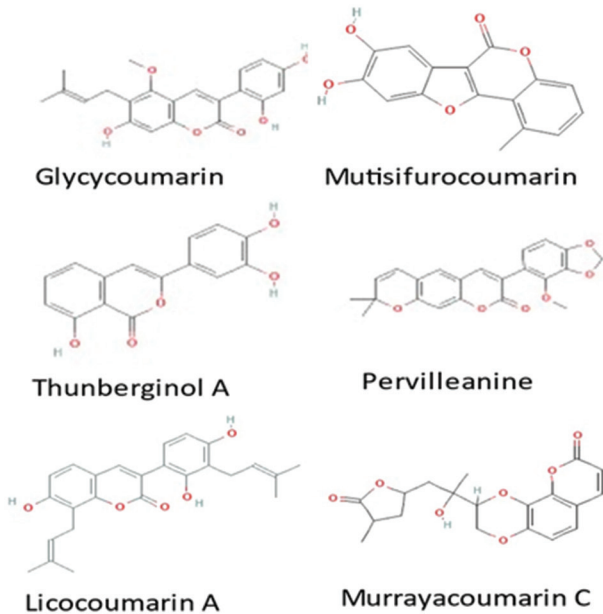


Fig. 1: 2D structure of top coumarin derivatives

a member of the ginger family, *Zingiberaceae*. Curcumin has sparked a lot of attention in the last couple of decades as an anti-inflammatory and anticancer drug. These qualities are ascribed to the curcumin structure's essential components. Curcumin's main mechanisms of action include triggering apoptosis and inhibiting tumor growth and invasion by suppressing a variety of cellular signaling pathways [11]. Curcumin has been proven in various trials to exhibit antitumor action against various tumors, revealing its ability to target a wide range of cancer cell lines. Despite all of the benefits described above, curcumin's usage is limited due to its low water solubility, which results in poor oral bioavailability and chemical stability.

In this present study, 50 coumarin and its derivatives were selected to determine their pharmacological properties and therapeutic efficacy against the endothelial and epidermal growth factor receptors implicated in the pathogenesis of various cancer. The therapeutic efficacy of the candidate coumarin derivatives was evaluated by employing the molecular docking technique and by analyzing their pharmacological properties.

**METHODS**

**Retrieval of ligands**

Secondary metabolites such as Coumarin and its derivatives were chosen from phytochemical constituents of various plants based on

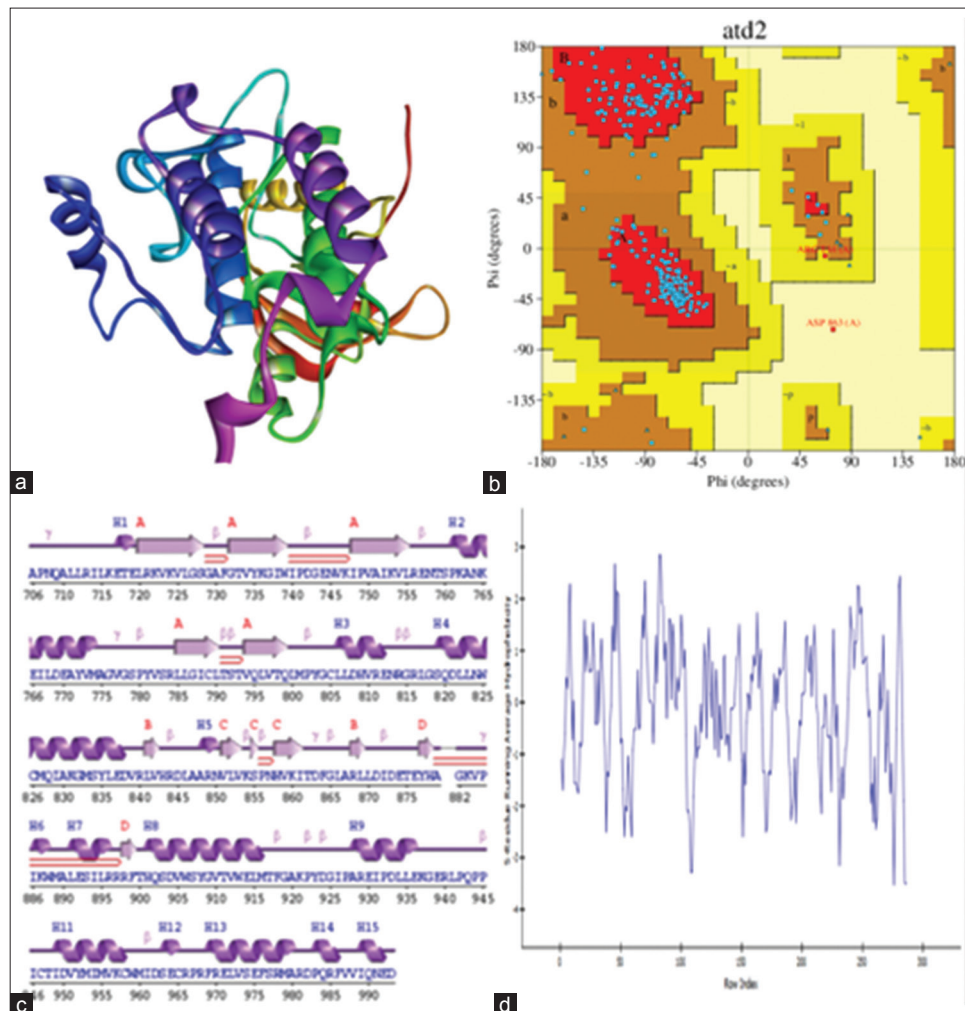


Fig. 2: Structural analysis of HER-2 protein (a) refers to purified HER-2 protein structure, in (b) we can observe the Ramachandra plot, (c) depicts the secondary structure of HER-2 and (d) shows, the hydrophobicity plot

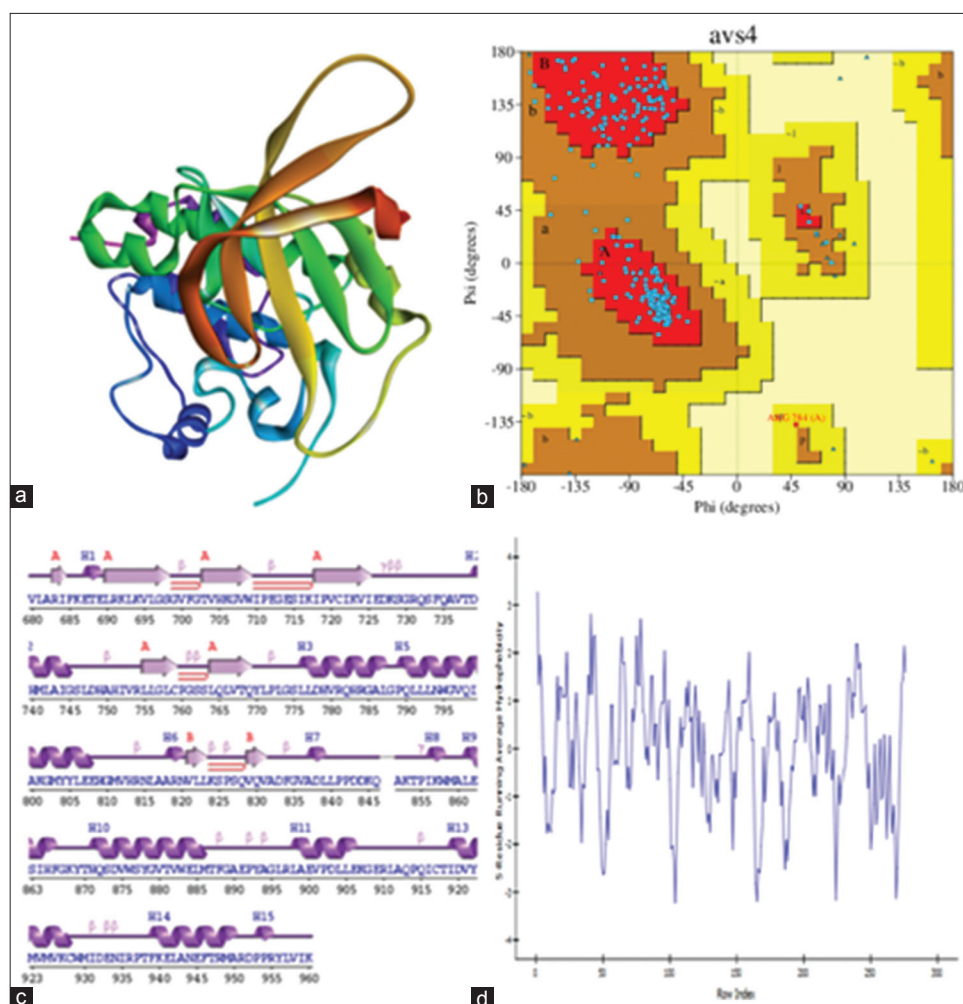


Fig. 3: Structural analysis of HER-3 protein (a) pertains to the purified HER-3 protein structure, (b) depicts the Ramachandra plot for HER-3, (c) shows the secondary protein structure, and (d) portrays the hydrophobicity plot

Table 1: Knapsack Id, name, PubChem Id, and the canonical smiles of the top 6 ligands chosen

Knapsack Id	Metabolites	PubChem CID	Canonical SMILES
C00010040	Glycycoumarin	5317756	<chem>CC(=CCC1=C(C2=C(C=C1O)OC(=O)C(=C2)C3=C(C=C(C=C3)O)O)OC)C</chem>
C00010060	Mutisifurocoumarin	3081083	<chem>CC1=C2C(=CC=C1)OC(=O)C3=C2OC4=CC(=C(C=C43)O)O</chem>
C00015274	Thunberginol A	5321948	<chem>C1=CC2=C(C(=C1)O)C(=O)OC(=C2)C3=CC(=C(C=C3)O)O</chem>
C00019150	Pervilleanine	11014334	<chem>CC1(C=CC2=C(O1)C=C3C(=C2)C=C(C(=O)O3)C4=C(C5=C(C=C4)OC5)OC)C</chem>
C00019315	Licocoumarin A	5324358	<chem>CC(=CCC1=C(C=CC(=C1O)C2=CC3=C(C(=C(C=C3)O)CC=C(C)C)OC2=O)O)C</chem>
C00030796	Murrayacoumarin C	11473870	<chem>CC1CC(OC1=O)CC(C)(C2COC3=C(O2)C4=C(C=C3)C=CC(=O)O4)O</chem>

Table 2: Binding affinity of coumarin derivatives toward the target proteins

Ligand	Binding affinity			
	HER-2	HER-3	VEGFR-2	VEGFR-3
Glycycoumarin	✖	-9.2	✖	-7.9
Mutisifurocoumarin	-10.1	✖	-10.3	✖
Thunberginol A	✖	-9.2	-10.8	✖
Pervilleanine	✖	✖	-12.2	-7.9
Licocoumarin A	-11.0	-8.7	✖	✖
Murrayacoumarin C	-11.6	✖	✖	-7.5

their anti-cancer capabilities. 50 coumarin derivatives from KNApSack-3D (<http://knapsack3d.sakura.ne.jp/index.html>) were included in

the current study [12]. The canonical SMILES, PubChem CID, and two-dimensional (2D) models of these compounds in SDF format were retrieved through the PubChem database (<https://pubchem.ncbi.nlm.nih.gov/>) [13].

#### Protein retrieval and purification

The three-dimensional crystal structure of endothelial growth factors including HER (HER2-3pp0 and HER3-6op9), VEGFR (VEGFR2-4bsj and VEGFR3-3vhe) was downloaded from Research Collaboratory for structural bioinformatics protein data bank (PDB) (<https://www.rcsb.org/>) in the .pdb format [14]. All the proteins were resolved using the X-ray diffraction method. The resolution of each protein is as follows: Human HER2 (2.25 Å) (Fig. 2a), HER3 (2.50 Å) (Fig. 3a), Human VEGFR2 (1.55 Å) (Fig. 4a), and VEGFR-3 (2.50 Å) (Fig. 5a). The missing residues in the protein structures were modeled using the SWISS-MODEL webserver (<https://swissmodel.expasy.org/>) [15]. The proteins were purified before docking by eliminating the heteroatoms,

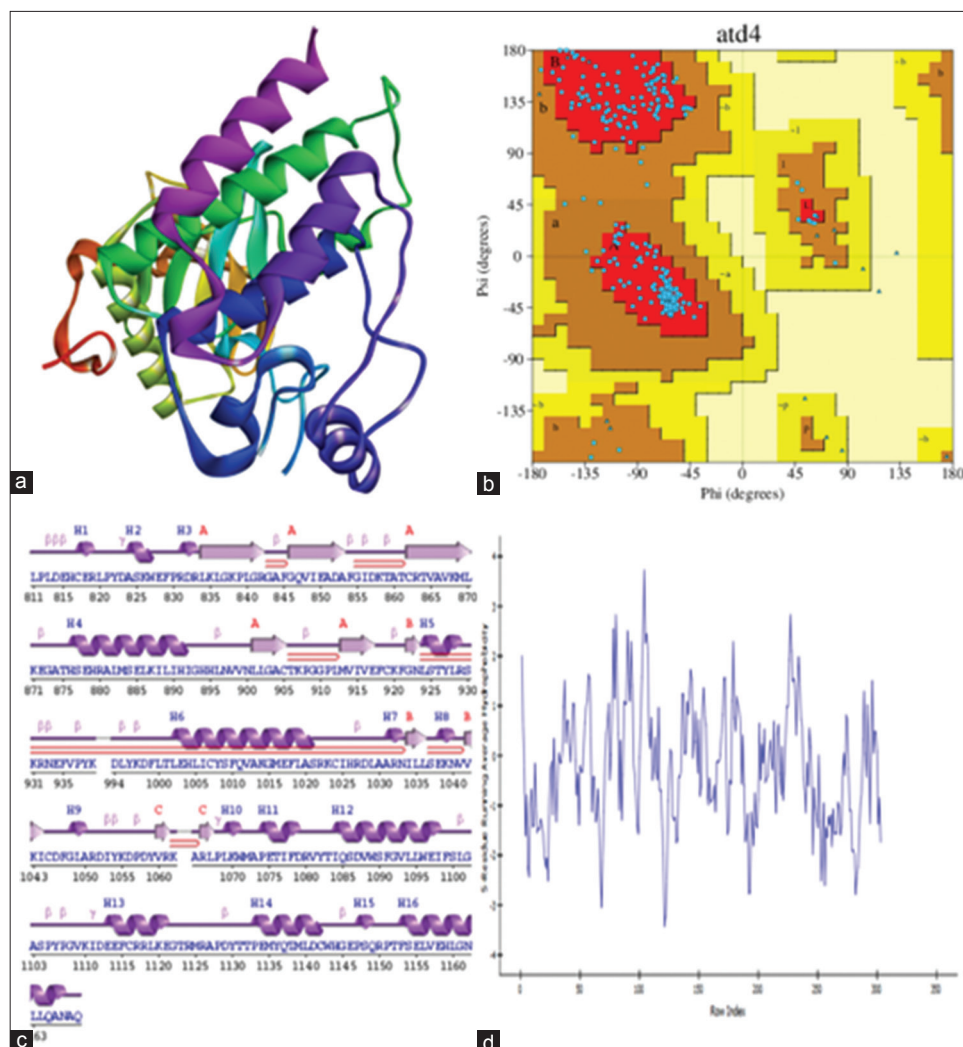


Fig. 4: Structural analysis of VEGFR-2 protein (a) relates to the purified protein structure of VEGFR-2, (b) represents the Ramachandra plot, (c) depicts the secondary protein structure, and (d) shows the VEGFR-2 hydrophobicity plot.

Table 3: Physicochemical properties of the top coumarin derivatives

PubChem ID	MW	nHA	nHD	nRot	nRing	MaxRing	nHet	nRig	Flex	TPSA	LogS	LogD	LogP
5317756	368.13	6	3	4	3	10	6	19	0.211	100.13	-3.351	3.353	4.538
3081083	282.05	5	2	0	4	17	5	21	0	83.81	-4.413	2.963	3.504
5321948	270.05	5	3	1	3	10	5	18	0.056	90.9	-3.627	2.837	3.155
11014334	378.11	6	0	2	5	14	6	27	0.074	67.13	-6.241	4.097	4.649
5324358	406.18	5	3	5	3	10	5	20	0.25	90.9	-3.21	3.721	6.486
11473870	360.12	7	1	3	4	14	7	23	0.13	95.2	-3.533	1.481	1.902

Table 4: Medicinal chemistry properties of the top Coumarin derivatives

PubChem id	QED	Pains	Lipinski	Fsp3	SAScore
5317756	0.474	0	Accepted	0.19	2.796
3081083	0.381	1	Accepted	0.062	2.561
5321948	0.591	1	Accepted	0	2.343
11014334	0.617	0	Accepted	0.227	2.981
5324358	0.379	0	Accepted	0.24	2.987
11473870	0.661	0	Accepted	0.474	4.404

Table 5: Absorption properties of the top coumarin derivatives

PubChem ID	Caco-2	MDCK	Pgp-inh	Pgp-sub	HIA	F (30%)
5317756	-4.834	1.27E-05	0.038	0.679	0.012	0.842
3081083	-4.954	1.34E-05	0.004	0.989	0.024	0.998
5321948	-4.879	1.20E-05	0.003	0.484	0.013	0.999
11014334	-4.777	2.15E-05	0.999	0.000	0.003	0.045
5324358	-4.875	1.63E-05	0.693	0.340	0.010	0.536
11473870	-4.775	3.14E-05	0.973	0.001	0.005	0.519

ligand group, and water molecules, and retaining only the A chains from the crystal structure of the proteins and polar hydrogens were added to the purified structures in the BIOVIA Discovery Studio software [16]. The purified structures of the proteins were further saved as .pdb files.

**Validation of protein structure**

The Ramachandran plot is used to assess the quality of a protein based on the torsion angles (Psi and Phi) in a protein structure. Ramachandran plot statistics show how many amino acid residues

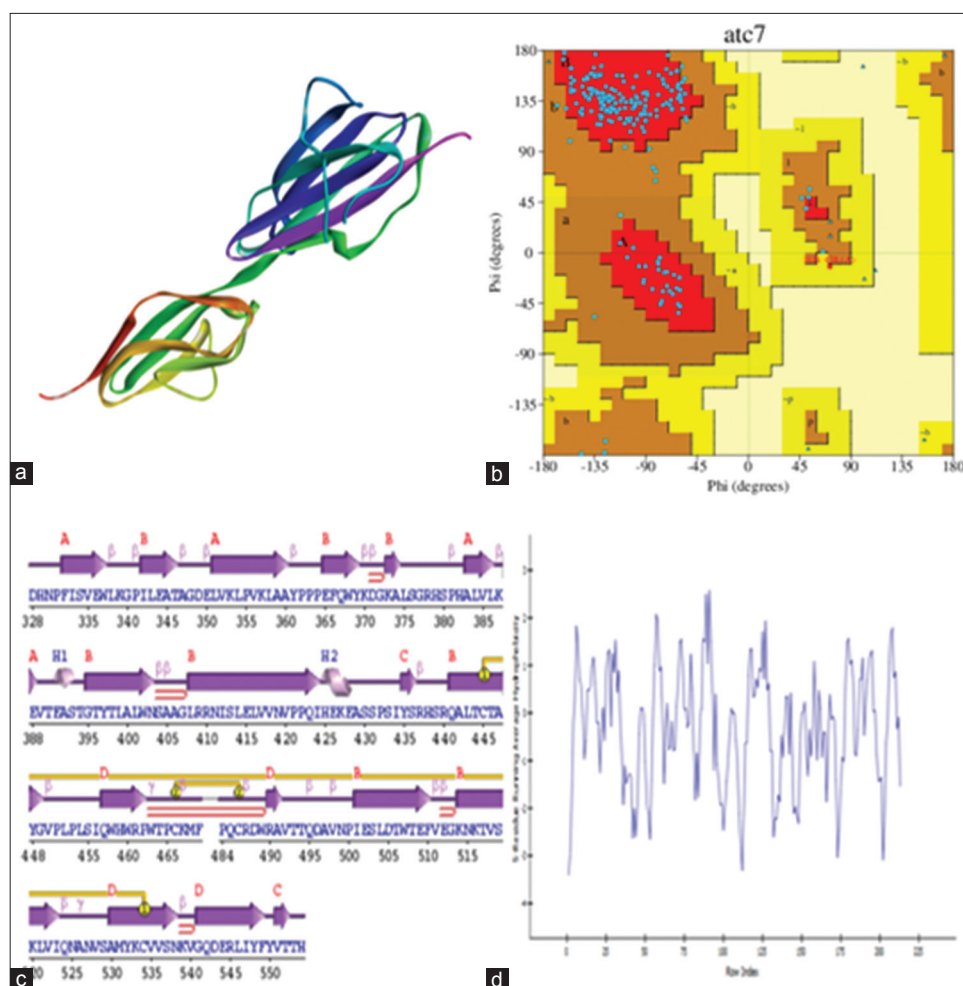


Fig. 5: Structural analysis of VEGFR-3 protein (a) represents the purified protein structure, (b) shows the Ramachandra plot, (c) depicts the secondary protein structure, and (d) illustrates the hydrophobicity plot

Table 6: Distribution properties of the top coumarin derivatives

PubChem ID	BBB	PPB (%)	VDss	Fu (%)
5317756	0.008	95.75	0.548	5.28
3081083	0.014	92.84	0.579	11.30
5321948	0.019	98.56	0.394	2.40
11014334	0.024	97.80	0.451	2.45
5324358	0.008	92.67	0.651	6.61
11473870	0.148	87.71	0.901	14.86

were identified in the favorable, allowed, and disallowed regions [17]. A hydrophilicity plot quantifies the amount of hydrophobicity or hydrophilicity of amino acids in a protein. The saved purified proteins files were used to obtain the Ramachandran plot and secondary structure of a protein using PDB sum generate (<http://www.ebi.ac.uk/thornton-srv/databases/pdbsum/Generate.html>) and hydrophobicity chart from BIOVIA discovery Studio software [18]. The target proteins were subjected to pathway analysis in the Reactome web server (<https://reactome.org/>).

#### Molecular docking

In this research, the primary investigative method used is Molecular Docking. PyRx is a virtual screening application that may be used in computational drug development to test chemical libraries against potential therapeutic targets [19]. The molecular docking of the 50 screened ligands was performed using the PyRx software's Molecular docking engine.

The ligands were docked with target proteins independently using PyRx software. Purified proteins were uploaded into PyRx as a macromolecule, and plant phytochemicals were added as ligands. Energy minimization was performed by applying the universal force field and the loaded ligands were converted into .pbqt format. The following grids were generated for each target protein, HER2 (Center X:12.4760 Y:21.6974 Z:34.0754; and Dimensions (angstrom) X:59.8607 Y:47.4074 Z:57.7324), HER3 (Center X:47.400 Y:18.307 Z:1.7267; and Dimensions (angstrom) X: 25.0000 Y:25.0000 Z:25.0000), VEGFR2 (Center X:21.505 Y:1.0559 Z:3.4527; and Dimensions (angstrom) X:51.1373 Y:53.9594 Z:57.0219), VEGFR3 (Center X:18.1577 Y:55.5238 Z:2.7953; and Dimensions (angstrom) X:81.9706 Y:64.9948 Z:58.7563). The ligands were docked with the target proteins and the corresponding docking interactions were evaluated based on the binding affinity. In PyRx the ligands take 9 different conformational changes to attain the best binding scores. The binding affinity corresponding to zero root mean square deviation (RMSD) values was appraised as the best docking conformation as they demonstrate the least binding scores among all the conformations. The top five conformations with the least binding affinity were selected as the best binding complex for each target protein. The docked ligand structures were extracted as .pdb files and the interaction was visualized in DS BIOVIA Discovery Studio.

#### Visualization

The output (docked structures) from PyRx was visualized using the structure visualization tool BIOVIA discovery studio software. The best-binding conformations were retrieved in .pdb format and viewed with

Table 7: Distribution properties of the top coumarin derivatives

PubChem ID	hERG	DILI	Ames	FDAMDD	Carcinogenicity	IGC50	LC <sub>50</sub>
5317756	0.032	0.899	0.032	0.643	0.055	4.983	5.734
3081083	0.003	0.985	0.458	0.899	0.489	4.342	5.168
5321948	0.028	0.948	0.211	0.223	0.362	4.756	5.248
11014334	0.116	0.91	0.047	0.892	0.924	4.579	5.583
5324358	0.015	0.933	0.061	0.096	0.108	5.013	6.389
11473870	0.029	0.946	0.034	0.662	0.917	3.77	4.072

hERG: The human ether-a-go-go related gene, DILI: Drug-induced liver injury, AMES: The Ames test for mutagenicity, FDAMDD: The maximum recommended daily dose, carcinogenicity, and 96-h fathead minnow LC<sub>50</sub> were examined

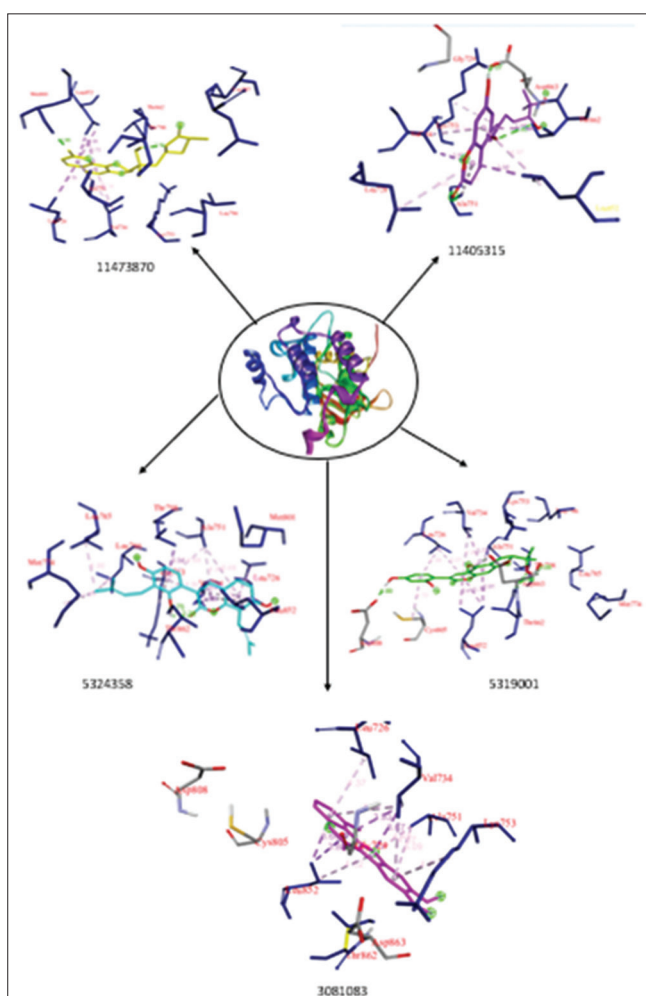


Fig. 6: 3D interactions of top ligands interacting with HER-2

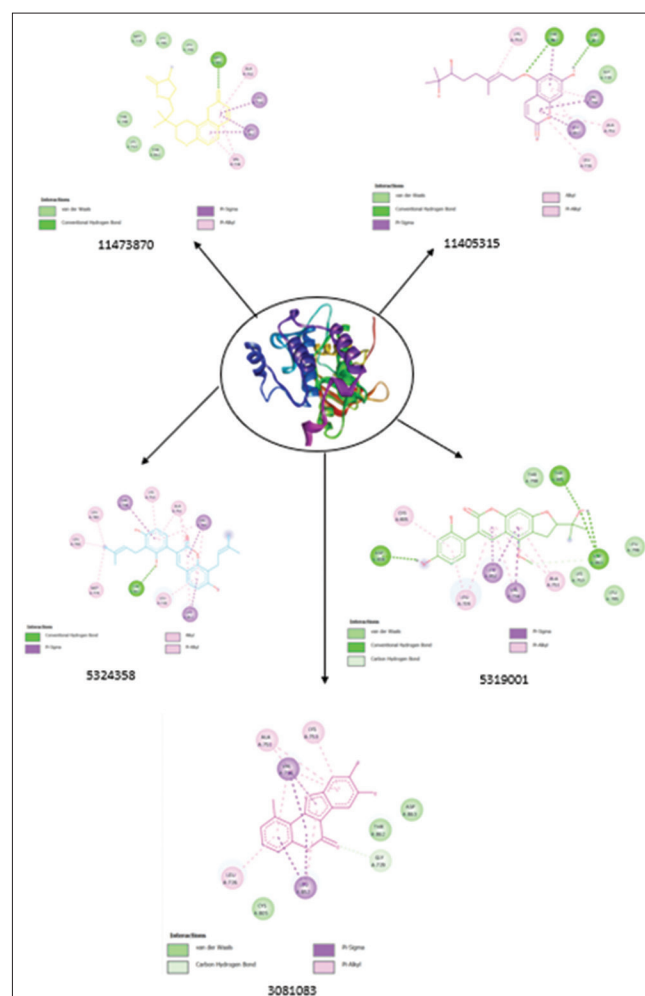


Fig. 7: 2D interactions of top ligands interacting with HER-2

BIOVIA Discovery Studio Visualizer. The non-bond interactions and the two-dimensional and three-dimensional models were investigated.

#### Physiochemical studies (ADMET screening)

The ADMET analysis facilitates the process of drug discovery by evaluating the attributes such as physiochemical properties, medicinal chemistry, absorption, distribution, and toxicity ADMET properties are fundamental in identifying drug-likeness properties and determining pharmacological efficacy as a possible candidate for medicinal development. ADMET analysis was performed using ADMETlab 2.0, an online server (<https://admetmesh.scbdd.com/>) [20]. From the docking results, the ligands with the best binding affinity were selected for ADMET analysis. The canonical SMILES of the top six ligands were retrieved from PubChem and were subjected to ADMET evaluation in the ADMETlab 2.0 webserver.

## RESULTS

### Selection of phytochemicals

Coumarin is known to portray a significant inhibitory role in the pathogenesis of various cancers and tumors. 50 coumarin and its derivatives, were chosen from KnapSack-3D to produce a suitable therapeutic candidate as shown in Fig. 1. Based on docking results, the 2D structures of the top 6 ligands with best binding affinity against the 4 proteins were obtained from PubChem. Using BIOVIA, the structures were viewed as shown in Table 1.

### Protein structure analysis

#### Ramachandra plot and Ramachandran plot statistics

PDBsum generate was used to produce the Ramachandran plot of HER-2, HER-3, VEGFR-2, and VEGFR-3 as shown in Figs. 2b-5b, respectively.

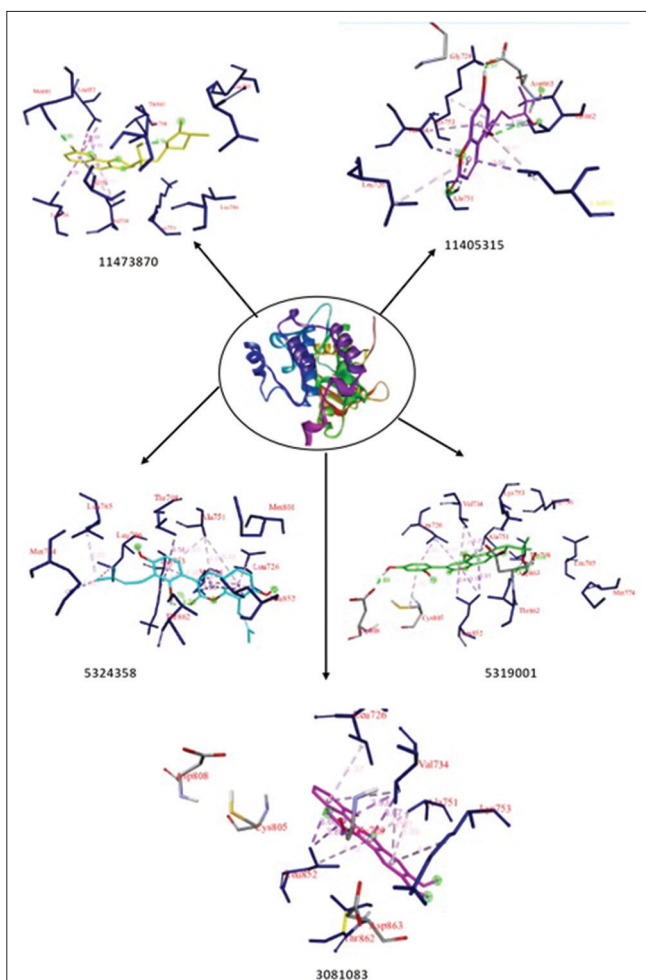


Fig. 8: 3D interactions of top ligands interacting with HER-3

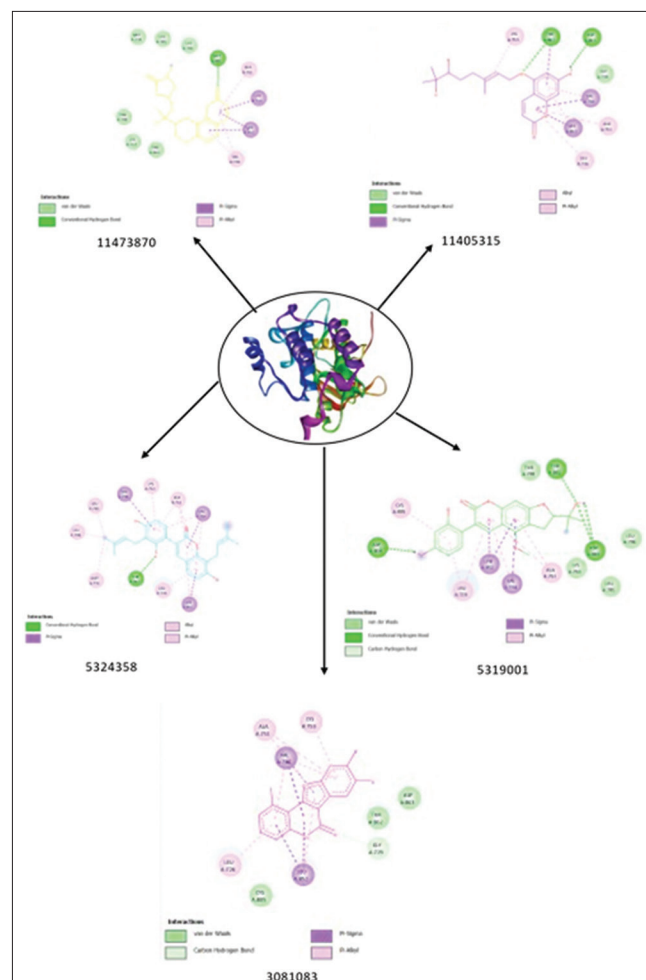


Fig. 9: 2D interactions of top ligands interacting with HER-3

• HER-2

The purified 3D structure of HER 2 has 91.6% of its residues in the most favored regions of the Ramachandran plot, 7.6% in additional allowed regions, 0.4% in generously allowed regions, and 0.4% in disallowed regions, according to the Ramachandran plot statistics.

• HER 3

Whereas, 91.9% of the residues in the purified 3D structure of HER 3 are in the most favored areas, 7.6% are in additional allowed regions, 0.4% are in generously allowed regions, and 0.0% are in disallowed regions.

• VEGFR-2

Likewise, VEGFR-2 contains 91.6% of its residues in the most favored areas, 8.4% in additional allowed regions, 0.0% in generously allowed regions, and 0.0% in disallowed regions.

• VEGFR-3

However, the Ramachandran plot statistics implied that the purified 3D structure of VEGFR-3 has 89.7% of its residues in the most favored regions, 9.7% of its residues in additional allowed regions, 0.5% of its residues in the generously allowed regions, and 0.0% of its residues in disallowed regions of the Ramachandran plot.

These statistics data validate that the modeled 3D structures are a good quality model.

*Secondary structure*

PDBsum was used to investigate the secondary structure of the 4 selected proteins namely, HER-2, HER-3, VEGFR-2, and VEGFR-3 as depicted in Figs. 2c-5c, respectively.

• HER-2

The PDBsum findings for protein secondary structure prediction are 4 sheets, 5 beta hairpins, 5 beta bulges, 11 strands, 15 helices, 16 helix-helix, 19 beta turns, and 4 gamma turns. The structure contains 286 residues in total.

• HER-3

However, for HER3 the PDBsum data shows 2 sheets, 4 beta hairpins, 3 beta bulges, 8 strands, 15 helices, 12 helix-helix, 19 beta turns, and 2 gamma turns. The structure constitutes 276 residues in total.

• VEGFR-2

In the case of VEGFR-2, The PDBsum results depicted are 3 sheets, 6 beta hairpins, 5 beta bulges, 10 strands, 16 helices, 12 helix-helix interacts, 25 beta turns, and 3 gamma turns. The structure comprises 303 residues in total.

• VEGFR-3

Finally, the PDBsum outputs for VEGFR-3 protein are 4 sheets, 5 beta hairpins, 5 beta bulges, 17 strands, 2 helices, 21 beta turns, 2 gamma turns, and 2 disulfides. There are 213 residues in all in the structure.

*Hydrophobicity plot*

The hydrophobicity plots of the HER-2, HER-3, VEGFR-2, and VEGFR-3 were investigated using the BIOVIA discovery studio software, as shown in Figs. 2d-5d, respectively.

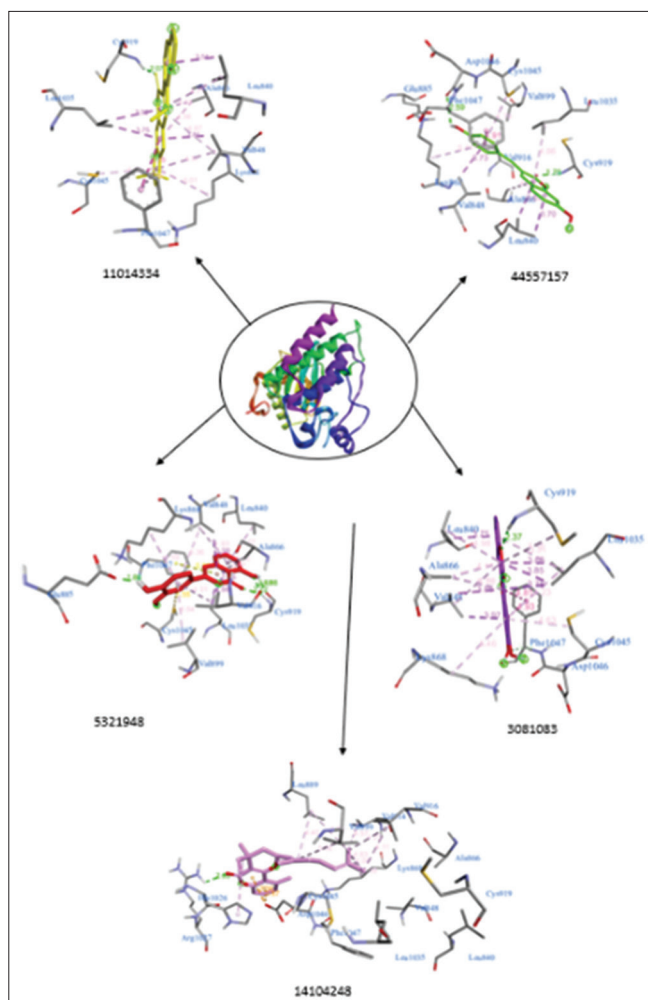


Fig. 10: 3D interactions of top ligands interacting with VEGFR-2

#### Molecular docking and visualization

In this docking study, fifty ligands were docked in PyRx software against four protein targets: HER-2, HER-3, VEGFR-2, and VEGFR-3. After docking was finished, the conformation with the lowest binding Affinity and RMSD was chosen as the best docking posture for the compounds.

After docking our ligands with targeted proteins, the binding affinity, RMSD/ub, and r/lb were recorded. Among 50 ligands screened, the top 6 ligands were selected with lowest binding affinity for each protein, namely, HER-2, HER-3, VEGFR-2, and VEGFR-3 as shown in Table 2.

The selected ligands were subjected to Visualization using Dassault Systems BIOVIA Discovery Studio Visualizer and the Two-dimensional as well as Three-dimensional models were acquired. Furthermore, information about the category and type of interaction along with the bond distance for the corresponding amino acid residues in the ligand was also obtained.

- Visualization of HER-2 (Figs. 6 and 7)
- Visualization of HER-3 (Figs. 8 and 9)
- Visualization of VEGFR-2 (Figs. 10 and 11)
- Visualization of VEGFR-3 (Figs. 12 and 13).

#### ADMET analysis

Six ligands, namely, Glycycoumarin (PubChem id: 5317756), Mutisifurocoumarin (PubChem ID: 3081083), Thunberginol A (PubChem ID: 5321948), Pervilleanine (PubChem ID: 11014334), Licocoumarin A (PubChem ID: 5324358), and Murrayacoumarin C (PubChem ID: 11473870) were screened for their physicochemical

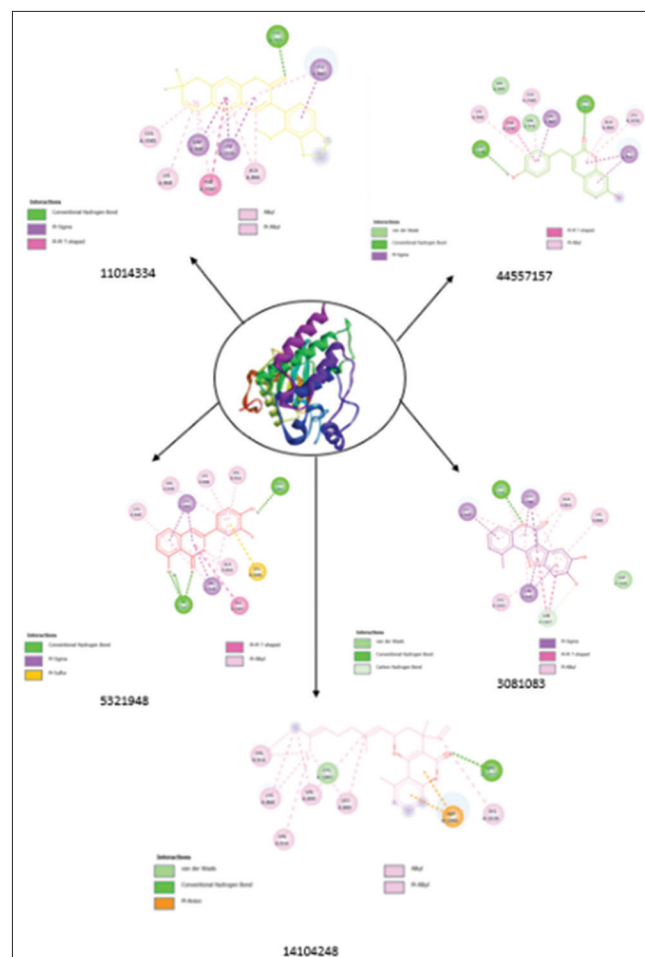


Fig. 11: 2D interactions of top ligands interacting with VEGFR-2

property, medicinal chemistry, absorption, distribution, and toxicity through a web tool called ADMETlab 2.0 as depicted in Tables 3-7.

#### DISCUSSION

Cancer metastasis has been thought to be the result of a series of biological events regulated by growth factor receptors and growth factor expression [21]. Cancer was not very frequent a century ago; nevertheless, its frequency has been increasing dramatically in recent decades, most likely due to our changing lifestyle, habits, and greater life expectancy. The situation is so dire that every fourth individual faces a lifelong risk of cancer. According to cancer registry statistics, it is believed that around 800,000 new cancer cases will be diagnosed in India each year [22].

The EGFR is one of the anticancer treatment targets for specific cancers such as non-small cell lung cancer, colorectal cancer, and head and neck squamous cell carcinoma. Since the identification of abnormally activated HER2 and HER3 causing resistance to EGFR inhibitors, extensive research on HER2- and HER3-targeting therapy has shown their benefits and limits. Human cancer genomic profiling has revealed recurrent somatic HER2 (ERBB2) and HER3 (ERBB3) mutations, which often arise in the absence of gene amplification 1-3. Mutations in HER2 are concentrated in the extracellular, transmembrane, and kinase domains. HER3 mutations, on the other hand, are concentrated largely in the extracellular domain and, to a lesser extent, in the kinase domain [23,24]. The VEGF and its receptor (VEGFR) have been shown to play key roles not only in physiology but also in most pathological angiogenesis, such as cancer. VEGF-A regulates angiogenesis and vascular permeability by activating two receptors, VEGFR-1 and

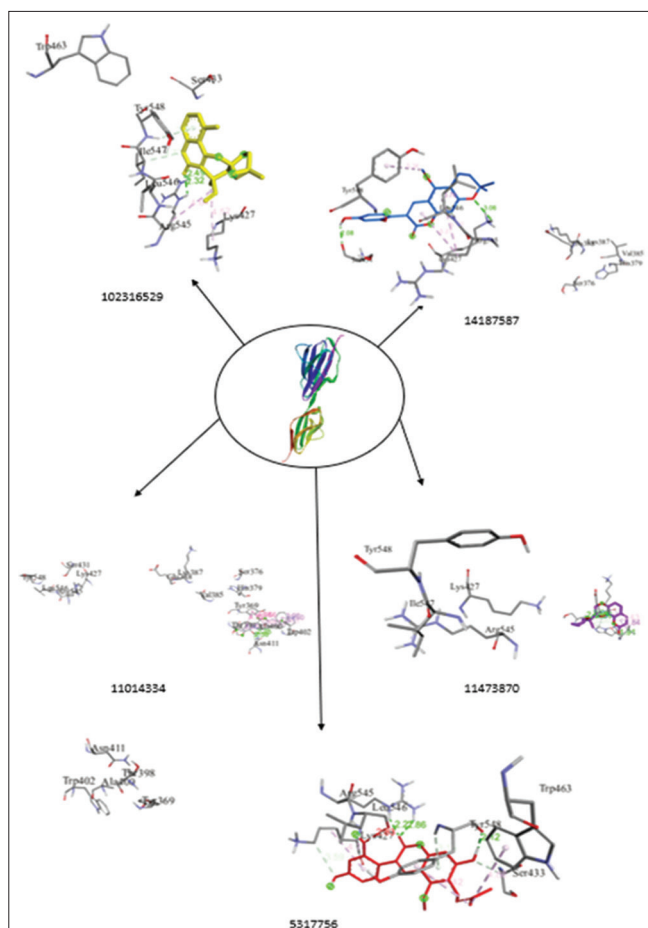


Fig. 12: 3D interactions of top ligands interacting with VEGFR-3

VEGFR-2, VEGF-C/VEGF-D and its receptor, VEGFR-3, on the other hand, primarily govern lymph angiogenesis [25]. VEGFR2 is the most common RTK that mediates VEGF signaling in endothelial cells and causes VEGF-mediated angiogenesis. Although the expression of these receptors was once assumed to be restricted to endothelial cells, it is now recognized that the majority of these receptors are expressed by a variety of tumor types and that their expression corresponds with clinical characteristics [26].

Curcumin (diferuloylmethane) is a polyphenol extracted from the *C. longa* plant. Curcumin has been used for millennia in Ayurvedic medicine because it is non-toxic and has a variety of therapeutic properties [27]. Curcumin has recently been proven to have anti-cancer capabilities as a result of its influence on a variety of biological pathways. Curcumin has been shown to decrease tumor development in several cancers. Curcumin also affects a variety of growth factor receptors and cell adhesion molecules, which are involved in tumor formation, angiogenesis, and metastasis [28]. Curcumin has been used as a nutritional supplement for millennia and is regarded as pharmacologically safe. Numerous research has shown that curcumin is both beneficial and safe. Curcumin's potential advantages as an anti-cancer drug have been examined in several pre-clinical and clinical investigations. Curcumin's anti-carcinogenic action is extremely promising, according to *in-vitro* and pre-clinical research, with its activity as an anti-cancer that can disrupt numerous pathways. Because of potential photochemotherapy and therapeutic implications in cancer, both natural and synthetic coumarin derivatives are gaining interest. For instance, Coumarins from *M. exotica* (Murrayacoumarin C) have been shown in studies to exhibit effective cytotoxicity against malignant cells [29]. Previous research evaluated Glycycoumarin's (GCM) anti-liver cancer action in both *in vitro* and *in vivo* models and discovered

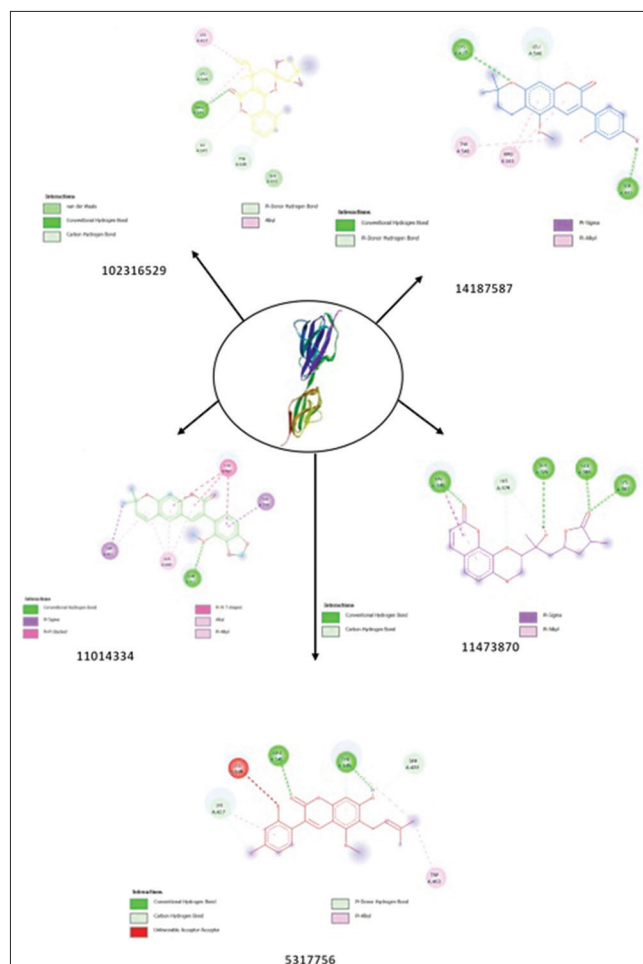


Fig. 13: 2D interactions of top ligands interacting with VEGFR-3

for the 1<sup>st</sup> time that GCM had potent activity against liver cancer as demonstrated by inhibition of cell growth and inducing apoptosis *in vitro* and tumor reduction *in vivo*. GCM was able to bind to and inactivate the oncogenic kinase T-LAK cell-originated protein kinase (TOPK), which then activated the p53 pathway. studies confirmed GCM as a novel active component that contributed to licorice's anti-cancer action, and TOPK might be a viable target for hepatocellular carcinoma therapy [30]. Whereas, methanolic licorice extract and its derived component, licocoumarin, have been shown to induce BCL<sub>2</sub> phosphorylation and arrest the G2/M cycle in cancer cell lines, along with triggering apoptosis in human monoblastic leukemia U937 cells.

In this study, 50 coumarin derivatives were selected based on their pharmacological applications. The ligands Murrayacoumarin C, Licocoumarin A, Licofuranocoumarin, Mutisifurocoumarin, and Murrayacoumarin A had the lowest binding affinity against the targeted protein HER-2 and hence were selected for further visualization. Ligands namely Sagecoumarin, Phyllocoumarin, Glycycoumarin, Thunberginol A, and Licocoumarin A had a higher binding affinity of -9.4, -9.3, -9.2, -9.2, and -8.7, respectively, with HER-3 were chosen. The ligands Pervilleanine, Thunberginol A, Anemarcoumarin A, Mutisifurocoumarin, and Triptiliocoumarin were selected for VEGFR-2 whereas, Pervilleanine, Glycycoumarin, Cycloethiliacoumarin, Murrayacoumarin C and Isoglycycoumarin for VEGFR-3 were selected based on their binding affinity score. These interactions were visualized using Dassault Systems BIOVIA Discovery Studio.

An overall analysis of the 2D structure of the top 5 ligands involved in docking with HER-2 (Fig. 7) revealed the implication of ALA:751, LEU:726, LEU:852, VAL:734, THR:862, and LYS753 as most common

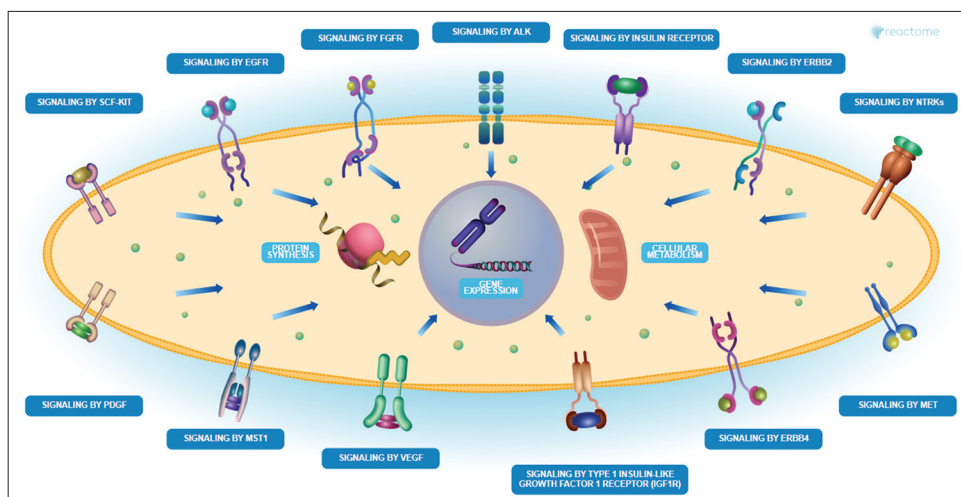


Fig. 14: Visualization of ERBB2 (HER-2), ERBB3 (HER-3), FLT4 (VEGFR-3), and KDR (VEGFR-2) genes involved in various pathways

amino acids. Whereas the examination of the 2D structures of the top 5 ligands docked with HER-3 (Fig. 9) indicated the presence of LYS:723, VAL:704, CYS:721, ALA:832, and LEU:822 as the most prevalent amino acids. However, the evaluation of the 2D structures of the top 5 ligands docked with VEGFR-2 (Fig. 11) showed the involvement of CYS:1045 and LYS:868 as the most common amino acids. Finally, the analysis of the 2D structures of the top 5 ligands docked with VEGFR-3 (Fig. 13) demonstrated the presence of zero amino acids as the most prevalent amino acids.

The results from the Reactome web server showed that the proteins were involved in various signaling pathways, downstream signal transduction, and others but most entities were seen in the RTK pathway as shown in Fig. 14. RTK activity affects several important activities, including cell growth and survival. However, RTK dysregulation has been observed in a broad variety of malignancies and has been demonstrated to link with the development and progression of various cancers. As a result, RTK has emerged as an appealing therapeutic target [31].

Further, *in silico* testing of the top six compounds predicted drug-likeness and ADMET characteristics. Pervilleanine and Mutisifurocoumarin have the least solubility. The TPSA of the six top ligands is optimum, indicating the compounds' efficacy in terms of membrane permeability. Murrayacoumarin C has a relatively low Clog P compared to others, indicating that it has strong hydrophilicity and may be easily absorbed by the cell, suggesting drug effectiveness. Lipinski filter criteria: H bond donors 5, H bond acceptors 10, and molecular weight in the range of 150–500 g/mol. The Lipinski filter analysis demonstrates that all of the phytochemicals in the table have potential drug characteristics. In comparison to other compounds, Murrayacoumarin C is the most attractive, whereas Licocoumarin A is the least attractive compound. Since all of the compounds have a low SAS score, they may be easy to synthesize. Murrayacoumarin C has a sufficient number of sp<sup>3</sup> hybridized carbons when compared to other ligands. Furthermore, because the drug must pass through the gastrointestinal membrane before reaching the systemic circulation, caco-2 cell permeability is utilized as an indicator for an appropriate candidate drug molecule, and human intestinal absorption of an oral drug is required for its apparent efficacy. All six ligands were anticipated to pass through caco-2 and be absorbed by the human intestine. In terms of predicting P-glycoprotein efflux from the cell, Glycycoumarin, Mutisifurocoumarin, and Thunberginol are anticipated to block p-glycoprotein, while Pervilleanine, Licocoumarin A, and Murrayacoumarin C may act as p-glycoprotein substrates. Papp values of MDCK cell lines are used to measure the effectiveness of chemical absorption into the body and to determine the influence of the blood-brain barrier, and all six substances demonstrate poor permeability. Murrayacoumarin C may

be able to reach its target location in high to moderate doses owing to its high capacity to bind to plasma proteins. Given that they are predicted to permeate the blood-brain barrier, all of the chemicals may potentially reach the CNS (BBB). Glycycoumarin, Mutisifurocoumarin, Licocoumarin A, and Murrayacoumarin C have a high proportion of unbound plasmas, allowing them to efficiently cross cellular membranes or diffuse. All six compounds are thought to have a suitable VD. Over the last 50 years, drug-induced liver damage has been the most prevalent safety issue associated with medication withdrawal from the market. Based on the scores, all of the compounds are non-toxic to liver cells, and daily doses are not hazardous to humans. Mutisifurocoumarin has the least ability to generate mutations among the six ligands, and Licocoumarin A is a weak carcinogen. The LC<sub>50</sub> of the top six ligands is less than the ideal score.

## CONCLUSION

According to the results of this study, the ligand Murrayacoumarin C has the best binding affinity for HER-2 (–11.6) and VEGFR-3 (–7.5), whereas Mutisifurocoumarin ligand has the lowest binding affinity towards HER-2 (–10.1) and VEGFR-2 (–10.3). Thunberginol A, on the other hand, has the best binding affinity for HER-3 (–9.2) and VEGFR-2 (–10.8), whereas Glycycoumarin has the lowest binding affinity towards HER-3 (–9.2) and VEGFR-3 (–7.9). Licocoumarin A has a good binding affinity toward both human endothelial receptors, HER-2 (–11) and HER-3 (–8.7) and Pervilleanine has the lowest binding affinity towards both the vascular endothelial receptors, VEGFR-2 (–12.2) and VEGFR-3 (–7.9), as shown in Table 2. *In vitro* studies can be employed to further study these compounds.

## ACKNOWLEDGMENT

I would like to thank Ms. Susha Dinesh for her guidance in undertaking the current project. I thank BioNome (<https://bionome.in/>) for offering computational facilities and help in scientific research services.

## REFERENCES

1. Ugai T, Sasamoto N, Lee HY, Ando M, Song M, Tamimi RM, *et al.* Is early-onset cancer an emerging global epidemic? Current evidence and future implications. *Nat Rev Clin Oncol* 2022;19:656-73.
2. Fidler MM, Gupta S, Soerjomataram I, Ferlay J, Steliarova-Foucher E, Bray F. Cancer incidence and mortality among young adults aged 20-39 years worldwide in 2012: A population-based study. *Lancet Oncol* 2017;18:1579-89.
3. Yan M, Schwaederle M, Arguello D, Millis SZ, Gatalica Z, Kurzrock R. HER2 expression status in diverse cancers: Review of results from 37,992 patients. *Cancer Metastasis Rev* 2015;34:157-64.
4. Loibl S, Gianni L. HER2-positive breast cancer. *Lancet* 2017;389:2415-29.

5. Vranić S, Bešlija S, Gatalica Z. Targeting HER2 expression in cancer: New drugs and new indications. *Bosn J Basic Med Sci* 2021;21:1-4.
6. Wang SL, Zhong GX, Wang XW, Yu FQ, Weng DF, Wang XX, *et al.* Prognostic significance of the expression of HER family members in primary osteosarcoma. *Oncol Lett* 2018;16:2185-94.
7. Liu X, Liu S, Lyu H, Riker AI, Zhang Y, Liu B. Development of effective therapeutics targeting HER3 for cancer treatment. *Biol Proced Online* 2019;21:5.
8. Claesson-Welsh L, Welsh M. VEGFA and tumour angiogenesis. *J Intern Med* 2013;273:114-27.
9. Klasa-Mazurkiewicz D, Jarzab M, Milczek T, Lipińska B, Emerich J. Clinical significance of VEGFR-2 and VEGFR-3 expression in ovarian cancer patients. *Pol J Pathol* 2011;62:31-40.
10. Su JL, Yen CJ, Chen PS, Chuang SE, Hong CC, Kuo IH, *et al.* The role of the VEGF-C/VEGFR-3 axis in cancer progression. *Br J Cancer* 2007;96:541-5.
11. Tomeh MA, Hadianamrei R, Zhao X. A review of curcumin and its derivatives as anticancer agents. *Int J Mol Sci* 2019;20:1033.
12. Nakamura K, Shimura N, Otabe Y, Hirai-Morita A, Nakamura Y, Ono N, *et al.* KnapSAcK-3D: A three-dimensional structure database of plant metabolites. *Plant Cell Physiol* 2013;54:e4.
13. Sayers EW, Beck J, Bolton EE, Bourexis D, Brister JR, Canese K, *et al.* Database resources of the national center for biotechnology information. *Nucleic Acids Res* 2021;49:D10-7.
14. Berman HM, Westbrook J, Feng Z, Gilliland G, Bhat TN, Weissig H, *et al.* The protein data bank. *Nucleic Acids Res* 2000;28:235-42.
15. Waterhouse A, Bertoni M, Bienert S, Studer G, Tauriello G, Gumienny R, *et al.* SWISS-MODEL: Homology modelling of protein structures and complexes. *Nucleic Acids Res* 2018;46:W296-303.
16. Panikar S, Shoba G, Arun M, Sahayarayan JJ, Nanthini AU, Chinnathambi A, *et al.* Essential oils as an effective alternative for the treatment of COVID-19: Molecular interaction analysis of protease (Mpro) with pharmacokinetics and toxicological properties. *J Infect Public Health* 2021;14:601-10.
17. Tam B, Sinha S, Wang SM. Combining Ramachandran plot and molecular dynamics simulation for structural-based variant classification: Using TP53 variants as model. *Comput Struct Biotechnol J* 2020;18:4033-9.
18. Laskowski RA. PDBsum: Summaries and analyses of PDB structures. *Nucleic Acids Res* 2001;29:221-2.
19. Dallakyan S, Olson AJ. Small-molecule library screening by docking with PyRx. *Methods Mol Biol* 2015;1263:243-50.
20. Xiong G, Wu Z, Yi J, Fu L, Yang Z, Hsieh C, *et al.* ADMETlab 2.0: An integrated online platform for accurate and comprehensive predictions of ADMET properties. *Nucleic Acids Res* 2021;49:W5-14.
21. Tanno S, Ohsaki Y, Nakanishi K, Toyoshima E, Kikuchi K. Human small cell lung cancer cells express functional VEGF receptors, VEGFR-2 and VEGFR-3. *Lung Cancer* 2004;46:11-9.
22. Roy PS, Saikia BJ. Cancer and cure: A critical analysis. *Indian J Cancer* 2016;53:441-2.
23. Hyman DM, Piha-Paul SA, Won H, Rodon J, Saura C, Shapiro GI, *et al.* HER kinase inhibition in patients with HER2-and HER3-mutant cancers. *Nature* 2018;554:189-94.
24. Yonesaka K. HER2-/HER3-targeting antibody-drug conjugates for treating lung and colorectal cancers resistant to EGFR inhibitors. *Cancers (Basel)* 2021;13:1047.
25. Shibuya M. Vascular endothelial growth factor (VEGF) and its receptor (VEGFR) signaling in angiogenesis: A crucial target for anti- and pro-angiogenic therapies. *Genes Cancer* 2011;2:1097-105.
26. Goel HL, Mercurio AM. VEGF targets the tumour cell. *Nat Rev Cancer* 2013;13:871-82.
27. Wilken R, Veena MS, Wang MB, Srivatsan ES. Curcumin: A review of anti-cancer properties and therapeutic activity in head and neck squamous cell carcinoma. *Mol Cancer* 2011;10:12.
28. Muninggar L, Widjiati W, Yuliatu I, Askandar B, Hartono P. Effects of curcumin on vascular endothelial growth factor expression on *Rattus norvegicus* cervical cancer xenograft model. *Indones J Cancer* 2019;12:95.
29. He SD, Yang XT, Yan CC, Jiang Z, Yu SH, Zhou YY, *et al.* Promising compounds from *Murraya exotica* for cancer metastasis chemoprevention. *Integr Cancer Ther* 2017;16:556-62.
30. Song X, Yin S, Zhang E, Fan L, Ye M, Zhang Y, *et al.* Glycycomarin exerts anti-liver cancer activity by directly targeting T-LAK cell-originated protein kinase. *Oncotarget* 2016;7:65732-43.
31. Takeuchi K, Ito F. Receptor tyrosine kinases and targeted cancer therapeutics. *Biol Pharm Bull* 2011;34:1774-80.